
Learning Personalized Models of Human Behavior in Chess

Reid McIlroy-Young

University of Toronto

reidmcy@cs.toronto.edu

Russell Wang

University of Toronto

russell@cs.toronto.edu

Siddhartha Sen

Microsoft Research

sidsen@microsoft.com

Jon Kleinberg

Cornell University

kleinberg@cornell.edu

Ashton Anderson

University of Toronto

ashton@cs.toronto.edu

Abstract

Even when machine learning systems surpass human ability in a domain, there are many reasons why AI systems that capture human-like behavior would be desirable: humans may want to learn from them, they may need to collaborate with them, or they may expect them to serve as partners in an extended interaction. Motivated by this goal of human-like AI systems, the problem of predicting human actions — as opposed to predicting optimal actions — has become an increasingly useful task. We extend this line of work by developing highly accurate personalized models of human behavior in the context of chess. Chess is a rich domain for exploring these questions, since it combines a set of appealing features: AI systems have achieved superhuman performance but still interact closely with human chess players both as opponents and preparation tools, and there is an enormous amount of recorded data on individual players. Starting with an open-source version of AlphaZero trained on a population of human players, we demonstrate that we can significantly improve prediction of a particular player’s moves by applying a series of fine-tuning adjustments. The differences in prediction accuracy between our personalized models and unpersonalized models are at least as large as the differences between unpersonalized models and a simple baseline. Furthermore, we can accurately perform stylometry — predicting who made a given set of actions — indicating that our personalized models capture human decision-making at an individual level.

1 Introduction

The advent of machine learning systems that surpass human ability in various domains raises the possibility of humans learning from and productively interacting with them. However, such human-AI collaboration is made difficult by the fact that many machine learning systems behave very differently from humans. The actions, techniques, or styles that work well for AI may not translate to how humans operate. To bridge this gap, a natural idea is to focus on characterizing human behavior — instead of approximating optimal policies in a given domain, learning to approximate *human* policies. Developing an ability to model human behavior in this way could provide a path toward building algorithmic learning tools that can effectively guide people to performance improvements, or machine learning systems that humans can more easily collaborate with to achieve a shared goal.

In recent work, researchers have made progress towards this objective in an ideal model system: chess [4, 43]. Chess has a number of attractive properties as a domain to pursue these questions in. First, chess AI definitively surpassed human chess-playing ability in 2005, yet millions of people still play it. There are billions of games played online each year, in each of which people face dozens

of decision-making situations, and the actions they take and how long they take to make them are digitally recorded. And it has been a leading indicator in AI and machine learning for decades; most recently, AlphaZero revolutionized algorithmic game-playing with a novel deep reinforcement learning framework. In [43], McIlroy-Young et al. trained an AlphaZero-like framework on millions of human games to characterize human behaviour in chess, where the objective is to predict which move the player will make. By training several models, each on a subset of games limited to a coarse skill level, this approach captures human behavior in chess at different levels of strength.

Although this was an important step, the ultimate realization of human behavior characterization would be the ability to emulate at the individual level. A model that could faithfully capture a particular person’s actions would be of clear use for automating different forms of interaction with them, and potentially for teaching them how to improve. However, in chess just as in other domains such as medical diagnosis and text generation, extremely strong performance is often achieved by aggregating data over many people; it is far from clear whether the variation among individuals provides sufficiently distinctive signals to enable individualized models to do significantly better than these high-performance aggregate models.

In this paper, we build models of individual human behavior in chess that outperform the coarse skill-level models in [43] by a wide margin. We find that our personalized models predict the exact move a human will play in a real game 64% of the time, whereas the unpersonalised skill-level models only predict them 50% accurately. This is a larger gap than the difference between the unpersonalised models and a simple baseline of “predicting” moves by using standard chess engines — where move agreement typically only occurs when both the human and the engine play a correct move. Our personalized models are much more accurate than the skill-level models both over the whole course of a chess game, from well-trodden opening lines to the final moves before checkmate, and across the span of move quality, from accurate engine-approved moves to outright blunders.

We achieve this by applying recent fine-tuning and transfer learning methods to an open-source implementation of the AlphaZero framework and personalizing move predictions to individual players. We use chess as an application domain to demonstrate how to fine-tune a deep neural network to an individual person when there are hundreds of thousands of examples per person, a feature that has traditionally not been present in other domains.

We demonstrate that our models capture individual decision-making to such an extent that we can use them to perform a version of the “author attribution” task. Here, we are given a game or set of games, and aim to predict who played it. Given one side of a single game, we can correctly identify the player who was playing out of a pool of 450 candidate players 65% of the time. Given many games, we can identify the player perfectly — even when we only consider the conclusions of the games or only consider poor moves, suggesting that our models capture unique features of a player’s decision-making style.

2 Related Work

Our work applies methods that were mainly developed in the transfer learning literature, but are also closely related to imitation learning, domain adaptation, meta-learning, and multitask learning. In particular, we experiment with fine-tuning our model by freezing its bottom layers [48, 67, 75], initializing the top layers randomly versus starting from a pre-existing model [17], and varying the pre-existing model that we start with [11, 37]. We derive inspiration from computer vision tasks that specialize a pre-existing model (e.g. Resnet-50 [23, 26]) to a specific task [34, 41, 49, 56, 74], a method that has also been extended to many other domains, such as natural language processing [14, 31, 50, 53, 73, 75] and speech recognition [15, 33, 38, 72].

Many developments in transfer learning are geared towards dealing with data scarcity by minimizing the number of samples required [38, 58, 65]. One of our contributions is to map out which techniques work best when even personalized models are relatively data-rich, a less well-studied setting [54]. Other approaches include adding additional layers [68] or additional inputs [36].

Several other machine learning tasks are closely related to our problem. It could be cast as a meta-learning task [5, 20, 55, 56], with the goal of picking the closest model to each individual. Our goal of training a model on human behavior is reminiscent of imitation learning, although a key difference is that in our setup we are starting from already-superhuman AI and aiming to design more human-friendly models, whereas imitation learning models are generally aiming to improve by observ-

ing an expert [16, 29, 60, 70]. Finally, our results on identifying players draw on some of the earliest uses of neural networks in handwriting recognition [40] and performing stylometry [25, 51, 52, 57, 69].

Our application domain, chess, has been used as a model system for artificial intelligence [4, 42, 46] and understanding human behavior [7, 9, 10, 24, 63] for decades. A period of fervent work on computer chess culminated in Deep Blue defeating Garry Kasparov in 1997, but more recently the introduction of AlphaZero, a system using deep residual networks, revolutionized the state of the art [13, 43, 61]. While AlphaZero is designed to approximate optimal play in chess even more perfectly than its predecessors, we adapt it to characterize human play at an individual level. Recent papers have pursued similar goals in cooperative game-playing [8], card-playing [6], and chess [43].

3 Data and Background

Lichess. We use data from the largest open-source online chess platform, Lichess [18]. With over 50 million games played per month, and almost 2 billion games played in total, Lichess provides us with a large number of diverse chess players, some of whom have played tens of thousands of games each. Games are played at variety of set durations, ranging from long games with an hour or more for each player to think, to extremely quick games with only 15 seconds per player for the entire game. For our work we ignore the fastest games, as players tend to make many more mistakes, sometimes intentionally, in order to not run out of time. Most of our games are from the Blitz category, with 3 to 8 minutes per player per game. Each player has an Elo rating representing their skill level, which is derived from their results against other players on the platform. A player with a rating 200 points higher than their opponent is expected to win 75% of the time. As most players are rated between 1100 and 2000 on Lichess, we restrict our attention to these players only. Lichess also has a robust community with impressive capabilities to detect bots and cheaters who use chess engine assistance. Players are also encouraged to maintain a single continuous account. As a result, we are able to train models on hundreds of human players with over 40,000 games played each.

Data Breakdown. To collect our specific set of players to train personalized models on, we first assembled a dataset containing all games from January 2013 to March 2020, and excluded December of 2019 as a test set (for consistency with [43]). We then selected the 1010 players with the most games (excluding the fastest games) within our 1100–2000 rating range to comprise our dataset¹. For each player their games (all had above 40,000 games) were then randomly shuffled and divided into three sets, training (80%, mean of ~1,700,000 board-move pairs), validation (10%, ~210,000 pairs), and testing (10%, ~210,000 pairs). We divided each player into one of three sets: an exploration set of 10 players we use to perform our methodological analyses, a test set of 398 players we use to present our final results, and a “lockbox” set of 602 players we reserve for future analyses. Code to convert raw Lichess files into our final splits and further details such as exact game counts are available in the Supplemental Material, section A.1.

Leela and Maia. Our work builds on two chess engines projects. The first, Leela Chess Zero, is an open source implementation of the deep reinforcement learning system *AlphaZero Chess* [61, 62], and provides the code infrastructure that we leverage to build our models. Maia, the second, is a supervised learning adaptation of Leela that attempts to predict the next move the average player of a particular Elo level will make in given a specific chess position [43]. By considering the problem as a classification task, the computationally intensive self-play reinforcement learning training process [66] and Monte Carlos Tree Search during play [59] can be avoided, resulting in significant speed-ups. More importantly for our purposes, using MCTS for human move prediction is less effective than pure classification [43]. This is likely due to the difficulty of constructing a value function [47] for approximating a human policy, as opposed to using the probability of winning as the value to achieve superhuman performance in approximating an optimal policy.

¹We used the mean ELO of the last 10,000 games played.

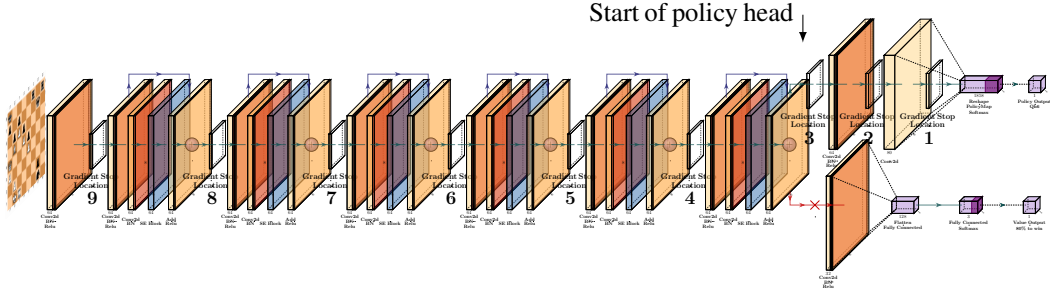


Figure 1: Our model architecture. Layers with learned weights are colored, and potential gradient stopping points are denoted by white layers. The lower value head is ignored during training.

4 Methodology

Our high-level approach is to take existing Maia models, which are designed to predict human moves at a particular skill level, and specialize them to predict the moves of an individual player using data from that player. This type of transfer learning can be carried out in myriad ways, which we organize through a logical sequence of design decisions that we explore in turn. The end result is a transfer learning methodology for creating a personalized model for any player, given a sufficient number of the player’s games. We create and evaluate personalized models for many players in our dataset in §5.1, then use these models to perform stylometry — uniquely identifying a player from their moves alone — in §5.2.

Since we start from an existing Maia model and train it on an individual player’s data, we first explore parameters required to define the mechanics of training, e.g., learning rate, batch size, and training steps. Then, instead of taking the entire Maia model verbatim, we explore which parts of it to copy, which parts to reinitialize, and which parts we allow the training process to adapt. Finally, we experiment with different starting Maia models to see if they influence the final accuracy of the personalized model; in the extreme, we train the Maia architecture from scratch solely using the individual player’s data.

During training we used a heavily modified version of the Leela Chess Zero training pipeline, as the data loading and tuning to training are significant. As their model is based on series of residual connections [28] between convolutional layers [39, 64] with ReLU activations [27, 45] and squeeze layers [32, 35], but without pooling layers, the core model design is not limited by this decision (see Figure 1 for a visualization of our architecture). The input representation is a 112-channel 8×8 board image representation², and there are two outputs: the predicted move (policy) and the probability of the active player winning the game (value). The predicted move is represented as a 1858-dimensional vector and we ignore the win prediction output in this work (our initial experiments showed it had no effect on our results). We keep the value head in our architecture for full compatibility with Leela, so that it is accessible to the broader chess engine community. The Leela training pipeline normally does not consider which player it is loading and requires full games for its data format, a compressed protocol buffer based binary [71]. Therefore, during training we discard the half of the data belonging to the other player in each game.

Training parameters. To explore the impact of various hyperparameter choices and design decisions, we conducted initial analyses on three players, two relatively high skill players and one low skill player (ratings near 1900, 1800 and 1100). Then we expanded our methodological experiments to our full suite of 10 training players. We evaluated both accuracy and loss (cross-entropy) on a small validation set of 20 players, along with training loss at frequent intervals. For each player, the move prediction accuracy is with respect to the final model on that player’s testing set of board positions (see §3). The optimizer used for all training was the Tensorflow Keras [2, 12] stochastic gradient descent and momentum optimizer.

In our initial experiments, we found a batch size of 256 and an initial learning rate of 0.01 followed by two reductions by factors of 10 during training to be optimal. We further divided the training batches into 64-element ghost batches [30] to shrink the generalization gap, reducing the impact of a large batch size. Almost all models stopped showing improvements after 130,000 steps, so we used 150,000 steps for the final training.

²12 layers, one per piece, make up a single board, and the last 8 boards are provided as input, with the other 16 layers including other metadata, e.g. if the active player is white.

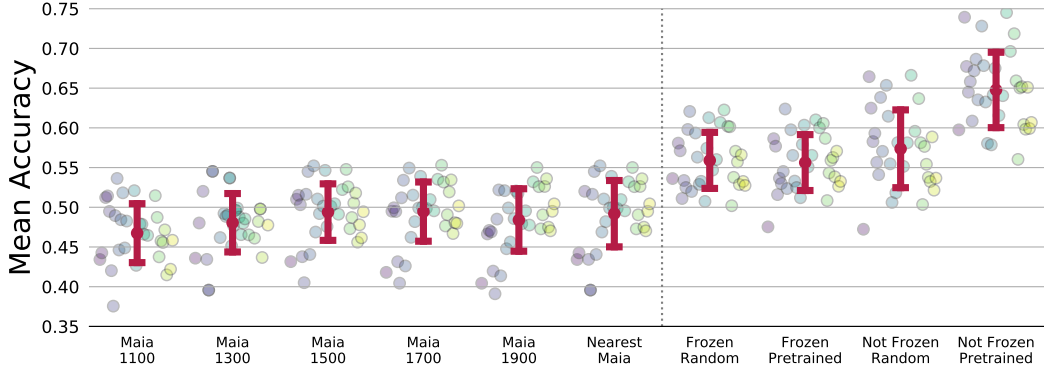


Figure 2: Accuracy on train and validation sets by model choice. Nearest Maia is the Maia with the closest trained Elo to the target player. Points are coloured and ordered by the player’s Elo, from low to high, left to right. Error bars show one standard deviation.

Depth of gradient flow. The two most important strategies we explored, in line with previous work, were freezing the top layers of our deep residual network, and either initializing weights randomly or with a preexisting model. We tested freezing our network at every reasonable location (all the white layers in Figure 1), and generally found that the deeper the gradients flowed the better performance we achieved (see full results in the Supplement, section A.2). Our initial experiments also generally showed that initializing our model with Maia’s weights also tended to give a boost at deeper stopping locations.

Model Choice. As previous work found that the Maia models best predict players at the rating level they were trained on, we expected the choice of which Maia we start with to also show this pattern (there is a different Maia model for each rating level [43]). Surprisingly, however, our experiments showed that our move prediction accuracy for a particular player doesn’t vary much with the choice of Maia we start with (i.e. we saw a 3% improvement from the worst model to the best in final accuracy; see Supplement for full details, section A.2.3). We also tried randomly initialization weights, which had a significant negative effect scaling with the depth of the stop. Introducing small amounts of Gaussian noise to the weights before training also had no effect or negative effects, depending on the amount of noise. Therefore, for the rest of the paper we start from Maia 1900, the model trained on the highest-Elo population of players.

Final Tuning. As a result of these preliminary analyses, we conducted a full experiment on our 10-player training set and 20-player validation set of all 4 combinations of freezing vs. not freezing and initializing weights randomly or starting from Maia 1900 weights. In this test, we chose to freeze at the most natural location — where the two outputs diverge (location 3 in Figure 1). The accuracy on each player’s testing data is shown in Figure 2. *Frozen* and *Not Frozen* refer to whether we stop the gradients at location 3 or let them propagate all the way through the model, and *Random* and *Pretrained* refer to whether we initialize the weights randomly or from Maia 1900.

As shown in Figure 1, all four of our personalized configurations significantly improve on the Maia baselines. We find that the best configuration, by a wide margin, is *Not Frozen, Pretrained* — where the gradients propagate through the entire network, and we initialize the weights with Maia 1900. Therefore, the *Not Frozen, Pretrained* architecture is our final model, and we now turn to presenting our results.

5 Results

We apply our transfer learning methodology to specialize the baseline Maia model (Maia 1900) to the 398 different players in our player test set. We use 90% of the target players’ games to train their personalized models, and evaluate them on the remaining 10% (the “test set”). Here, we show the results for the original task of predicting the target player’s moves (§5.1), as well as a different stylometry task of identifying the player given only a subset of their moves (§5.2).

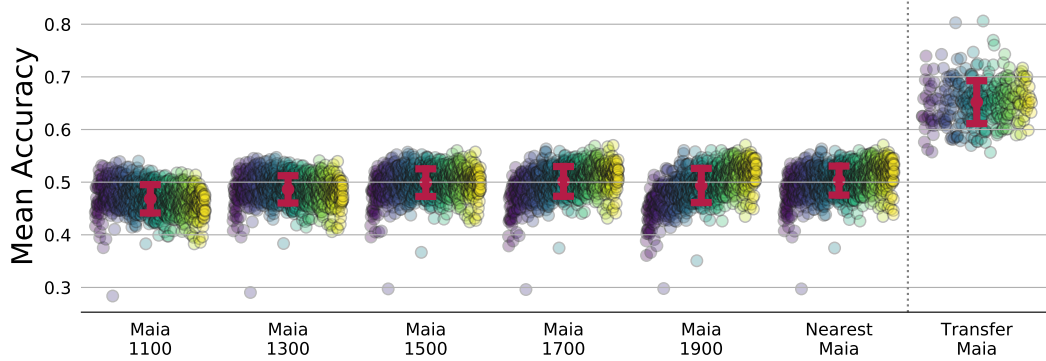


Figure 3: Mean move prediction accuracy of our personalized model versus Maia models on target players’ test set games. Target players are color-coded by Elo rating level from left (lower rating) to right (higher rating). Nearest Maia is the Maia whose training level is closest to the target player’s rating. Error bars show one standard deviation (the standard error is microscopic). The personalized model achieves significantly higher accuracy than the best Maia model on every player.

5.1 Move Prediction Accuracy

We evaluate how accurately our personalized models predict the moves of their target players on their test sets. For comparison, we also evaluate the Maia models on the test set; as we observed, these models represent the state-of-the-art in human move prediction, but they can only predict at coarse skill levels (Elo ratings). Thus we expect the Maia model whose training level is closest to a target player’s rating, which we call the “nearest” Maia, to have the highest accuracy. Figure 3 shows the results, where the target players are color-coded by their rating and ordered from left (lower rating) to right (higher rating). As expected, Maia’s accuracy increases as its training level approaches the target player’s rating, which for example explains the downward tilt of Maia 1100 and the upward tilt of Maia 1900. This replicates the main result of McIlroy-Young et al. [43]. The “Nearest Maia” column combines the top performing Maia models per player. In contrast, our personalized models outperform all Maia models by a sizable margin, achieving 13% higher accuracy on average than the top performing Maia model, per player.

That we can achieve higher move prediction accuracy through personalization is a result that is neither implied by nor expected based on the performance of Maia, which has enough difficulty predicting moves at coarse rating levels. To investigate the effect of this personalization, we also evaluate the personalized models on the original testing set used to evaluate Maia [43]. Specifically, we evaluate each personalized model on 1000 games from each rating level from 1100 to 1900. Not surprisingly, the personalized models perform uniformly worse than Maia on this dataset, achieving a mean accuracy of 42%, which is almost 20% lower than their accuracy on their respective target players. Moreover, the drop in accuracy occurs almost immediately after training begins—within just 500 batches—whereas it takes much longer for the models to achieve the higher personalized accuracy numbers in Figure 3. In other words, our transfer learning methodology quickly loses accuracy on the original task but takes much longer to achieve good accuracy on the specialized task.

A plausible explanation for the higher accuracy of our models is that they are memorizing formulaic patterns in the opening play, or other easily predictable aspects of the target player’s style. To investigate this, we perform a finer analysis of model accuracy along different dimensions. Figure 4(a) shows how model accuracy varies as the move number in the game increases. While both the personalized models and Maia models benefit from the higher predictability of opening play, the benefit quickly diminishes as more moves are played. Despite these dynamics, personalized models achieve consistently superior accuracy by a significant margin throughout the entire game.

Figure 4(b) shows how model accuracy varies with the quality or “goodness” of the move being predicted. The goodness of a move is measured by the change in estimated win probability before and after the move, where win probability is calculated via an empirical procedure based on the position’s centipawn score, following the method of McIlroy-Young et al. [43]. The change is always negative because it is measured against optimal play (the strange jump at -0.12 is an artifact of win probability calculation, as explained in the figure). As the figure shows, both the personalized models and Maia

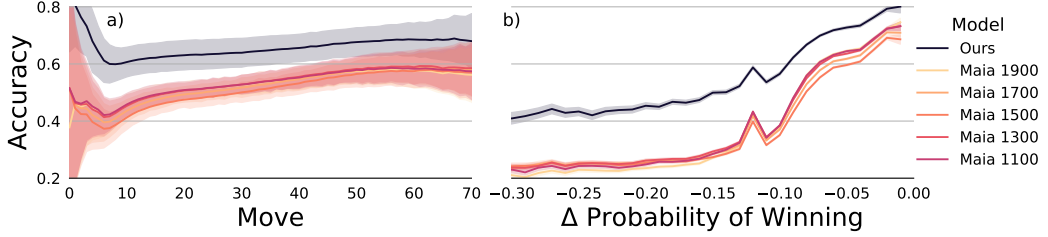


Figure 4: Mean move prediction accuracy of our personalized models versus Maia models as we vary (a) move number in the game (b) quality of the move. The jump in (b) is an artifact of the way win probability is calculated which causes -0.12 to appear 50% more frequently than its neighboring values.

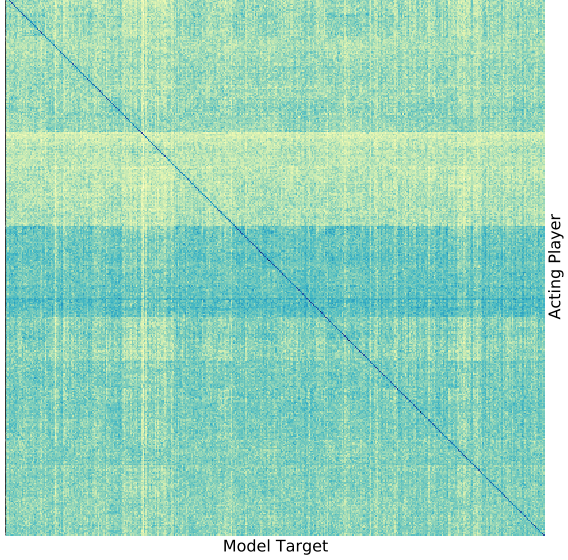


Figure 5: Accuracy of every personalized model (columns) evaluated on 4 games from every player’s test set (rows).

models can predict better moves with higher accuracy than worse moves, but the personalized models are consistently more accurate across all move qualities, by a significant margin. In fact, our models achieve only 0.015% higher accuracy on games won by the target player than those they lost. This versatility is a useful property for teaching purposes, because lost games are at least as instructive (and typically more instructive) than won games.

A distinguishing property of the personalized models compared to Maia is that their accuracy is largely independent of the target player’s rating in the range we examine (1100-1900 Elo). The R^2 of an ordinary least squares regression of accuracy against player rating is 0.004, which is negligible. This property may not hold across all rating levels, however: our preliminary attempts to create personalized models for Grandmasters did not yield the same accuracy gains as above. We conjecture that at the highest levels of play, it is more difficult for human-oriented models such as Maia and ours to achieve higher accuracy than chess engines like Stockfish or Leela, because the strongest players tend to play near-optimal moves which traditional chess engines are designed to predict.

5.2 Styliometry

Having created personalized models that achieve higher accuracy than non-personalized baselines, a natural question to ask is how unique these models are. In particular, can the personalized model of one player be used to predict the moves of another player? Figure 5 shows the accuracy of each personalized model (columns) on 4 games sampled from each of the 398 players (rows). The players are ordered using ward clustering [44], so players with more similar accuracy vectors are closer together. As the dark diagonal line shows, the model that achieves the highest accuracy for a player is

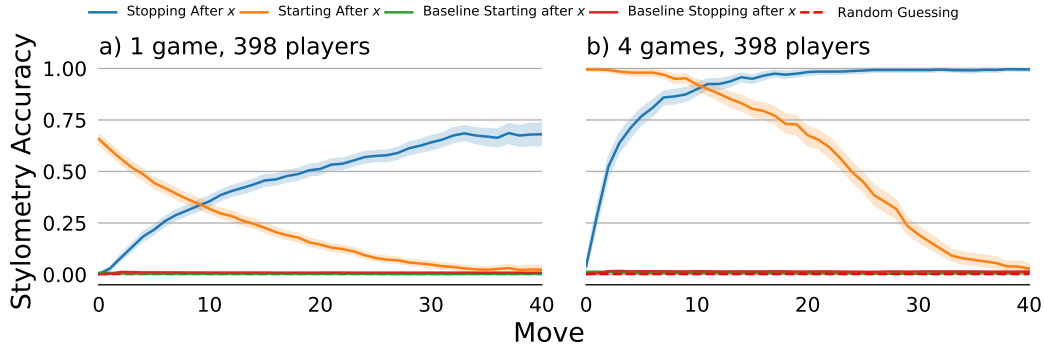


Figure 6: Stylometry accuracy (prediction accuracy of player identification) as a function of which moves the models are given, when we use (a) only one game, and (b) 4 games to determine the player. Baselines are present on both figures, but the differences from random guessing are not visibly evident. *Stopping after x* means that only moves before move x are considered, while *Starting after x* means only moves after move x are used.

indeed their personalized model. In addition, most of the models (96%) achieve their highest absolute accuracy when acting on their target player’s games.

This result has profound implications, because it means that we can uniquely identify a player by simply inspecting a few of their games—i.e., we can perform *stylometry*! The method is simple: given a player’s games, test each personalized model on those games and output the one with the highest move prediction accuracy. Since we know the personalized models perform poorly on games outside of the player set—recall that they achieve 42% accuracy on the original Maia testing set—we can also identify when a game has not been played by any of the players by using a simple accuracy threshold.

To examine these results more closely, we perform stylometry on a single game (sampled from the test set) and vary the subset of moves that are shown to the models. Figure 6(a) shows the results. If all moves from the beginning up to move x are shown, the accuracy converges quickly to 66%; conversely, starting at move x and proceeding to the end of the game degrades accuracy gradually from 68% to 2.5% (orange line). The discrepancy in the shapes of these curves suggests that the later moves of a game more uniquely identify a player than earlier moves of the game. As a baseline for stylometry, we train a Naive Bayes classifier (one for each game length) on the vector of centipawn losses incurred by each player on their training set games, and use this classifier to identify the most likely player given a game (and its associated centipawn loss vector). Though a reasonable style marker, this baseline achieves very poor accuracy compared to our personalized models, peaking at 1.4% which is only slightly better than random guessing. Other style markers may achieve better results, but finding a good style marker is difficult in general [21]. In effect, our personalized models serve as a proxy for style markers: by abstracting the differences between players through the move prediction task, we can perform stylometry without the need for explicit style markers.

By increasing the number of games provided to the models, we can dramatically boost our stylometry accuracy. Figure 6(d) shows that with just 4 games, accuracy converges very quickly to nearly 100%. To further investigate the effect of multiple games, we used a smaller set of 30 players (from §4) and gave the models access to 4,000 games from their test sets. The results are shown in the supplement, section A.3. Interestingly, the stylometry accuracy reaches and *stays* at 100% regardless of which subset of moves is shown to the models. For example, showing only move x from each of the 4,000 games results in 100% stylometry accuracy, provided x occurs after the very first few moves (e.g., move 3 and beyond).

Looking at the stylometry accuracy as a function of the change in win probability, we find that the most distinguishing moves are those with win probability change near -0.1 , which corresponds to a slight inaccuracy in chess. This suggests that small inaccuracies are a potentially good style marker for distinguishing players in chess.

6 Discussion

This work takes the next step in the quest to learn *human* policies, by building on the coarse, skill-level models of prior work to create personalized models for individual players. Our models can predict a player’s moves more accurately than any prior baseline, regardless of when the move occurs in a game or how good or bad it is. Our models capture enough individual behavior to allow us to perform near-perfect stylometry: given just a few games, we can uniquely identify the player from among a set of ~400 players.

An interesting challenge is to scale up our methodology along different dimensions: e.g., more players, more skill levels, and more time periods. For example, as we mentioned, creating accurate personalized models for the strongest players (Grandmasters) remains an elusive challenge. By developing these algorithmic tools, we hope to advance human learning and facilitate collaboration with AI systems, using chess as a model system.

Broader Impact

Chess has traditionally been an open, public ecosystem, with both online and offline games documented, uploaded, and made easily searchable to the public. Every game can be efficiently retrieved; every position can be efficiently matched against previous games; every individual player’s history can be easily viewed.

Our work relies entirely on this public data. Anyone can use our code and model architectures to reproduce any of our results. Although it would not increase their exposure, we anonymize the usernames and other identifying information of all players for whom we develop personalized models.

Just because chess is an open system, and our results do not increase this openness, does not mean that the current state of affairs is ethically sound, or that our results do not affect this soundness. One can argue, as others (e.g., the great Bobby Fischer) have attempted in the past, that a player’s games are their intellectual property and warrant protection. Historically, such cases have faced difficulty because a game involves two players, not just one.

The presence of superhuman chess engines has led to the occurrence of cheating during online gameplay. Our personalized models do not increase the effectiveness of cheating, because predicting an opponent’s next move is not as effective as knowing the optimal move to play (assuming the goal is to beat the opponent). However, our personalized models could be used to target practice training and practice with a specific player in mind, so as to increase the likelihood of defeating that player in a game. However, it is quite likely that the accuracy numbers of our models are not high enough to make such targeted practice effective.

Unlike our move prediction accuracy, our stylometry accuracy is extremely high (almost 100%). This has interesting implications. For example, our personalized models could be used to identify when an individual’s playing style has unexpectedly or sharply changed, which could help identify cases of cheating.

Since the data of a chess game consists of usernames and a sequence of moves, it does not seem likely that such data could generate models that are unfair or biased against protected attributes. However, the players we create personalized models for must have a sufficient number of online games, so to the extent that access to the Internet is biased by protected attributes, the subset of models we train will carry this bias.

We do not expect the openness of chess data to last forever. With the trend towards users demanding more control [3], getting more control [19], and creating policies and law to sanction such control [1], we expect chess data, and other online game data, to join this bandwagon. While such ownership will make investigations such as ours difficult (or perhaps infeasible), we believe that this is the right direction to pursue, and any lack in accessibility or feasibility of study can always be combated by ideas and innovations from the research community itself. Homomorphic encryption [22], or the ability to perform arbitrary computations over encrypted data, though still very impractical, is an example of this from a different domain.

References

- [1] European Commission [n.d.]. *2018 reform of EU data protection rules*. European Commission. https://ec.europa.eu/commission/sites/beta-political/files/data-protection-factsheet-changes_en.pdf
- [2] Martín Abadi, Ashish Agarwal, Paul Barham, Eugene Brevdo, Zhifeng Chen, Craig Citro, Greg S. Corrado, Andy Davis, Jeffrey Dean, Matthieu Devin, Sanjay Ghemawat, Ian Goodfellow, Andrew Harp, Geoffrey Irving, Michael Isard, Yangqing Jia, Rafal Jozefowicz, Lukasz Kaiser, Manjunath Kudlur, Josh Levenberg, Dandelion Mané, Rajat Monga, Sherry Moore, Derek Murray, Chris Olah, Mike Schuster, Jonathon Shlens, Benoit Steiner, Ilya Sutskever, Kunal Talwar, Paul Tucker, Vincent Vanhoucke, Vijay Vasudevan, Fernanda Viégas, Oriol Vinyals, Pete Warden, Martin Wattenberg, Martin Wicke, Yuan Yu, and Xiaoqiang Zheng. 2015. TensorFlow: Large-Scale Machine Learning on Heterogeneous Systems. <https://www.tensorflow.org/> Software available from tensorflow.org.
- [3] Alessandro Acquisti, Laura Brandimarte, and George Loewenstein. 2015. Privacy and human behavior in the age of information. *Science* 347, 6221 (2015), 509–514.
- [4] Ashton Anderson, Jon Kleinberg, and Sendhil Mullainathan. 2017. Assessing human error against a benchmark of perfection. *ACM Transactions on Knowledge Discovery from Data (TKDD)* 11, 4 (2017), 45.
- [5] Marcin Andrychowicz, Misha Denil, Sergio Gomez, Matthew W Hoffman, David Pfau, Tom Schaul, Brendan Shillingford, and Nando De Freitas. 2016. Learning to learn by gradient descent by gradient descent. In *Advances in neural information processing systems*. 3981–3989.
- [6] Hendrik Baier, Adam Sattaur, Edward J Powley, Sam Devlin, Jeff Rollason, and Peter I Cowling. 2018. Emulating human play in a leading mobile card game. *IEEE Transactions on Games* 11, 4 (2018), 386–395.
- [7] Tamal Biswas and Kenneth W Regan. 2015. Measuring Level-K Reasoning, Satisficing, and Human Error in Game-Play Data. In *2015 IEEE 14th International Conference on Machine Learning and Applications*. IEEE, Miami, FL, 941–947.
- [8] Micah Carroll, Rohin Shah, Mark K Ho, Tom Griffiths, Sanjit Seshia, Pieter Abbeel, and Anca Dragan. 2019. On the Utility of Learning about Humans for Human-AI Coordination. In *Advances in Neural Information Processing Systems*. 5175–5186.
- [9] Neil Charness. 1992. The impact of chess research on cognitive science. *Psychological research* 54, 1 (1992), 4–9.
- [10] William G Chase and Herbert A Simon. 1973. Perception in chess. *Cognitive psychology* 4, 1 (1973), 55–81.
- [11] Ken Chatfield, Karen Simonyan, Andrea Vedaldi, and Andrew Zisserman. 2014. Return of the devil in the details: Delving deep into convolutional nets. *arXiv preprint arXiv:1405.3531* (2014).
- [12] François Chollet et al. 2015. Keras. <https://keras.io>.
- [13] Johannes Czech, Moritz Willig, Alena Beyer, Kristian Kersting, and Johannes Fürnkranz. 2019. Learning to play the Chess Variant Crazyhouse above World Champion Level with Deep Neural Networks and Human Data. *arXiv preprint arXiv:1908.06660* (2019).
- [14] Andrew M Dai and Quoc V Le. 2015. Semi-supervised sequence learning. In *Advances in neural information processing systems*. 3079–3087.
- [15] Jun Deng, Zixing Zhang, Erik Marchi, and Björn Schuller. 2013. Sparse autoencoder-based feature transfer learning for speech emotion recognition. In *2013 humaine association conference on affective computing and intelligent interaction*. IEEE, 511–516.
- [16] Yiming Ding, Carlos Florensa, Pieter Abbeel, and Mariano Phielipp. 2019. Goal-conditioned imitation learning. In *Advances in Neural Information Processing Systems*. 15298–15309.

[17] Jeff Donahue, Yangqing Jia, Oriol Vinyals, Judy Hoffman, Ning Zhang, Eric Tzeng, and Trevor Darrell. 2014. Decaf: A deep convolutional activation feature for generic visual recognition. In *International conference on machine learning*. 647–655.

[18] Thibault Duplessis. 2019. Lichess. lichess.org. Accessed: 2019-10-09.

[19] Mica R Endsley. 2016. *Designing for situation awareness: An approach to user-centered design*. CRC press.

[20] Chelsea Finn, Pieter Abbeel, and Sergey Levine. 2017. Model-agnostic meta-learning for fast adaptation of deep networks. In *Proceedings of the 34th International Conference on Machine Learning-Volume 70*. JMLR.org, 1126–1135.

[21] Leon A Gatys, Alexander S Ecker, and Matthias Bethge. 2016. Image style transfer using convolutional neural networks. In *Proceedings of the IEEE conference on computer vision and pattern recognition*. 2414–2423.

[22] Craig Gentry. 2009. Fully homomorphic encryption using ideal lattices. In *Proceedings of the forty-first annual ACM symposium on Theory of computing*. 169–178.

[23] Daniel George, Hongyu Shen, and EA Huerta. 2018. Classification and unsupervised clustering of LIGO data with Deep Transfer Learning. *Physical Review D* 97, 10 (2018), 101501.

[24] Fernand Gobet and Herbert A Simon. 1996. Templates in chess memory: A mechanism for recalling several boards. *Cognitive psychology* 31, 1 (1996), 1–40.

[25] Alex Graves, Marcus Liwicki, Santiago Fernández, Roman Bertolami, Horst Bunke, and Jürgen Schmidhuber. 2008. A novel connectionist system for unconstrained handwriting recognition. *IEEE transactions on pattern analysis and machine intelligence* 31, 5 (2008), 855–868.

[26] Kaiming He, Ross Girshick, and Piotr Dollár. 2019. Rethinking imagenet pre-training. In *Proceedings of the IEEE International Conference on Computer Vision*. 4918–4927.

[27] Kaiming He, Xiangyu Zhang, Shaoqing Ren, and Jian Sun. 2015. Delving deep into rectifiers: Surpassing human-level performance on imagenet classification. In *Proceedings of the IEEE international conference on computer vision*. 1026–1034.

[28] Kaiming He, Xiangyu Zhang, Shaoqing Ren, and Jian Sun. 2016. Deep residual learning for image recognition. In *Proceedings of the IEEE conference on computer vision and pattern recognition*. 770–778.

[29] Jonathan Ho and Stefano Ermon. 2016. Generative adversarial imitation learning. In *Advances in neural information processing systems*. 4565–4573.

[30] Elad Hoffer, Itay Hubara, and Daniel Soudry. 2017. Train longer, generalize better: closing the generalization gap in large batch training of neural networks. In *Advances in Neural Information Processing Systems*. 1731–1741.

[31] Jeremy Howard and Sebastian Ruder. 2018. Universal language model fine-tuning for text classification. *arXiv preprint arXiv:1801.06146* (2018).

[32] Jie Hu, Li Shen, and Gang Sun. 2018. Squeeze-and-excitation networks. In *Proceedings of the IEEE conference on computer vision and pattern recognition*. 7132–7141.

[33] Zhen Huang, Sabato Marco Siniscalchi, and Chin-Hui Lee. 2016. A unified approach to transfer learning of deep neural networks with applications to speaker adaptation in automatic speech recognition. *Neurocomputing* 218 (2016), 448–459.

[34] Minyoung Huh, Pulkit Agrawal, and Alexei A Efros. 2016. What makes ImageNet good for transfer learning? *arXiv preprint arXiv:1608.08614* (2016).

[35] Forrest N Iandola, Song Han, Matthew W Moskewicz, Khalid Ashraf, William J Dally, and Kurt Keutzer. 2016. SqueezeNet: AlexNet-level accuracy with 50x fewer parameters and< 0.5 MB model size. *arXiv preprint arXiv:1602.07360* (2016).

[36] Jeremy Kawahara and Ghassan Hamarneh. 2016. Multi-resolution-tract CNN with hybrid pretrained and skin-lesion trained layers. In *International workshop on machine learning in medical imaging*. Springer, 164–171.

[37] Simon Kornblith, Jonathon Shlens, and Quoc V Le. 2019. Do better imagenet models transfer better?. In *Proceedings of the IEEE conference on computer vision and pattern recognition*. 2661–2671.

[38] Julius Kunze, Louis Kirsch, Ilia Kurenkov, Andreas Krug, Jens Johannsmeier, and Sebastian Stober. 2017. Transfer learning for speech recognition on a budget. *arXiv preprint arXiv:1706.00290* (2017).

[39] Yann LeCun, Bernhard Boser, John S Denker, Donnie Henderson, Richard E Howard, Wayne Hubbard, and Lawrence D Jackel. 1989. Backpropagation applied to handwritten zip code recognition. *Neural computation* 1, 4 (1989), 541–551.

[40] Yann LeCun, Léon Bottou, Yoshua Bengio, and Patrick Haffner. 1998. Gradient-based learning applied to document recognition. *Proc. IEEE* 86, 11 (1998), 2278–2324.

[41] Geert Litjens, Thijs Kooi, Babak Ehteshami Bejnordi, Arnaud Arindra Adiyoso Setio, Francesco Ciompi, Mohsen Ghafoorian, Jeroen Awm Van Der Laak, Bram Van Ginneken, and Clara I Sánchez. 2017. A survey on deep learning in medical image analysis. *Medical image analysis* 42 (2017), 60–88.

[42] John McCarthy. 1990. Chess as the Drosophila of AI. In *Computers, chess, and cognition*. Springer, New York, NY, 227–237.

[43] Reid McIlroy-Young, Siddhartha Sen, Jon Kleinberg, and Ashton Anderson. 2020. Aligning Superhuman AI and Human Behavior: Chess as a Model System. *arXiv preprint arXiv:2006.01855* (2020).

[44] Daniel Müllner. 2011. Modern hierarchical, agglomerative clustering algorithms. *arXiv preprint arXiv:1109.2378* (2011).

[45] Vinod Nair and Geoffrey E Hinton. 2010. Rectified linear units improve restricted boltzmann machines. In *Proceedings of the 27th international conference on machine learning (ICML-10)*. 807–814.

[46] Allen Newell, John Calman Shaw, and Herbert A Simon. 1958. Chess-playing programs and the problem of complexity. *IBM Journal of Research and Development* 2, 4 (1958), 320–335.

[47] Andrew Y Ng, Stuart J Russell, et al. 2000. Algorithms for inverse reinforcement learning.. In *Icml*, Vol. 1. 2.

[48] Maxime Oquab, Leon Bottou, Ivan Laptev, and Josef Sivic. 2014. Learning and transferring mid-level image representations using convolutional neural networks. In *Proceedings of the IEEE conference on computer vision and pattern recognition*. 1717–1724.

[49] Sinno Jialin Pan and Qiang Yang. 2009. A survey on transfer learning. *IEEE Transactions on knowledge and data engineering* 22, 10 (2009), 1345–1359.

[50] Matthew E. Peters, Mark Neumann, Mohit Iyyer, Matt Gardner, Christopher Clark, Kenton Lee, and Luke Zettlemoyer. 2018. Deep contextualized word representations. *CoRR* abs/1802.05365 (2018). arXiv:1802.05365 <http://arxiv.org/abs/1802.05365>

[51] Vu Pham, Théodore Bluche, Christopher Kermorvant, and Jérôme Louradour. 2014. Dropout improves recurrent neural networks for handwriting recognition. In *2014 14th International Conference on Frontiers in Handwriting Recognition*. IEEE, 285–290.

[52] Réjean Plamondon and Sargur N Srihari. 2000. Online and off-line handwriting recognition: a comprehensive survey. *IEEE Transactions on pattern analysis and machine intelligence* 22, 1 (2000), 63–84.

[53] Alec Radford, Karthik Narasimhan, Tim Salimans, and Ilya Sutskever. 2018. Improving language understanding by generative pre-training. *URL https://s3-us-west-2.amazonaws.com/openai-assets/researchcovers/languageunsupervised/languageunderstandingpaper.pdf* (2018).

[54] Colin Raffel, Noam Shazeer, Adam Roberts, Katherine Lee, Sharan Narang, Michael Matena, Yanqi Zhou, Wei Li, and Peter J Liu. 2019. Exploring the limits of transfer learning with a unified text-to-text transformer. *arXiv preprint arXiv:1910.10683* (2019).

[55] Aniruddh Raghu, Maithra Raghu, Samy Bengio, and Oriol Vinyals. 2019. Rapid learning or feature reuse? towards understanding the effectiveness of maml. *arXiv preprint arXiv:1909.09157* (2019).

[56] Maithra Raghu, Chiyuan Zhang, Jon Kleinberg, and Samy Bengio. 2019. Transfusion: Understanding transfer learning for medical imaging. In *Advances in Neural Information Processing Systems*. 3342–3352.

[57] Michael Revow, Christopher KI Williams, and Geoffrey E Hinton. 1996. Using generative models for handwritten digit recognition. *IEEE transactions on pattern analysis and machine intelligence* 18, 6 (1996), 592–606.

[58] Marcus Rohrbach, Sandra Ebert, and Bernt Schiele. 2013. Transfer learning in a transductive setting. In *Advances in neural information processing systems*. 46–54.

[59] Christopher D Rosin. 2011. Multi-armed bandits with episode context. *Annals of Mathematics and Artificial Intelligence* 61, 3 (2011), 203–230.

[60] Stefan Schaal. 1999. Is imitation learning the route to humanoid robots? *Trends in cognitive sciences* 3, 6 (1999), 233–242.

[61] David Silver, Thomas Hubert, Julian Schrittwieser, Ioannis Antonoglou, Matthew Lai, Arthur Guez, Marc Lanctot, Laurent Sifre, Dharshan Kumaran, Thore Graepel, et al. 2018. A general reinforcement learning algorithm that masters chess, shogi, and Go through self-play. *Science* (2018).

[62] David Silver, Julian Schrittwieser, Karen Simonyan, Ioannis Antonoglou, Aja Huang, Arthur Guez, Thomas Hubert, Lucas Baker, Matthew Lai, Adrian Bolton, et al. 2017. Mastering the game of go without human knowledge. *Nature* (2017).

[63] Herbert A Simon. 1977. The structure of ill-structured problems. In *Models of discovery*. Springer, 304–325.

[64] Karen Simonyan and Andrew Zisserman. 2014. Very deep convolutional networks for large-scale image recognition. *arXiv preprint arXiv:1409.1556* (2014).

[65] Qianru Sun, Yaoyao Liu, Tat-Seng Chua, and Bernt Schiele. 2019. Meta-transfer learning for few-shot learning. In *Proceedings of the IEEE Conference on Computer Vision and Pattern Recognition*. 403–412.

[66] Richard S Sutton and Andrew G Barto. 2018. *Reinforcement learning: An introduction*. MIT press.

[67] Nima Tajbakhsh, Jae Y Shin, Suryakanth R Gurudu, R Todd Hurst, Christopher B Kendall, Michael B Gotway, and Jianming Liang. 2016. Convolutional neural networks for medical image analysis: Full training or fine tuning? *IEEE transactions on medical imaging* 35, 5 (2016), 1299–1312.

[68] Chuanqi Tan, Fuchun Sun, Tao Kong, Wenchang Zhang, Chao Yang, and Chunfang Liu. 2018. A survey on deep transfer learning. In *International conference on artificial neural networks*. Springer, 270–279.

[69] Charles C. Tappert, Ching Y. Suen, and Toru Wakahara. 1990. The state of the art in online handwriting recognition. *IEEE Transactions on pattern analysis and machine intelligence* 12, 8 (1990), 787–808.

[70] Faraz Torabi, Garrett Warnell, and Peter Stone. 2019. Recent advances in imitation learning from observation. *arXiv preprint arXiv:1905.13566* (2019).

- [71] Kenton Varda. 2008. Protocol buffers: Google’s data interchange format. *Google Open Source Blog, Available at least as early as Jul 72* (2008).
- [72] Dong Wang and Thomas Fang Zheng. 2015. Transfer learning for speech and language processing. In *2015 Asia-Pacific Signal and Information Processing Association Annual Summit and Conference (APSIPA)*. IEEE, 1225–1237.
- [73] Jie Yang, Yue Zhang, and Fei Dong. 2017. Neural word segmentation with rich pretraining. *arXiv preprint arXiv:1704.08960* (2017).
- [74] Jason Yosinski, Jeff Clune, Yoshua Bengio, and Hod Lipson. 2014. How transferable are features in deep neural networks?. In *Advances in neural information processing systems*. 3320–3328.
- [75] Barret Zoph, Deniz Yuret, Jonathan May, and Kevin Knight. 2016. Transfer learning for low-resource neural machine translation. *arXiv preprint arXiv:1604.02201* (2016).

A Supplement

This section contains more detailed discussion of our hyperparameter search and two additional plots showing our stylometry work.

A.1 Source Code, Models, Data

A copy of our code and other files will be made available after the review period.

Data. The main data source for this work is the games database on *Lichess.org*, database.lichess.org. Each player’s information is given in Table 6 for the 398-player main dataset and in Table 5 for the 30-player validation set used for the model selection. Figure 7 shows how the all players are distributed by the number of games and Elo rating.

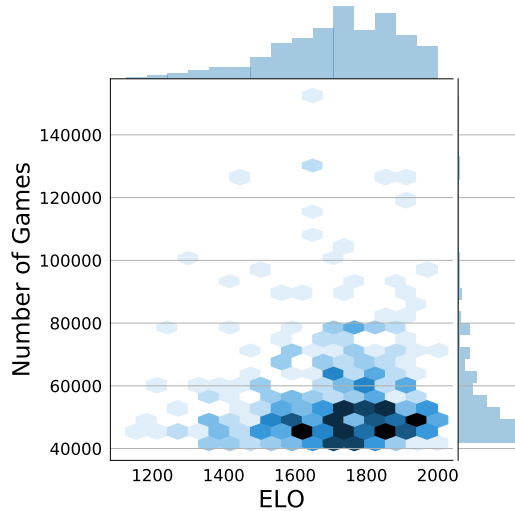


Figure 7: Players ELO and number of games, you can see that the density of players is higher at higher ELOs.

For each player, we constructed two holdout sets of games, with one to be used for model selection (validation set) and one to be used for final testing (test set). Note that the results shown in the main text for our large sample of 398 players never uses the validation sets during either training or testing.

A.2 Methodology Details

In this section, we will discuss the details of the methodological process we went through.

In our initial explorations of the parameter space, we selected 10 players at random from our whole set of highly-active players. In our final exploration detailed in the main text Section 4, we added an additional set of 20 players who were used for analysing the final four models. Table 5 lists all 30 players with the initial ten labeled as *train*.

Although we conducted our initial investigations on several players, for simplicity we will report results on a single player. Different players tend to have different baseline levels of predictability, i.e. one player could start at 0.45 accuracy on Maia and reach 0.61 on the final model, while another will start at 0.55 and reach 0.74. This means looking at the accuracy of multiple players is high variance, even though their gains in predictability are correlated. The player we report our results on has an Elo rating near 1900 and is number 25 in Table 5. They have 59,007 total games played, which we split into a training set with 47,207 games and a validation set with 5,900 games.

We report accuracy on the validation set. The accuracy is measured the same way as our results in the main text: the number of moves correctly predicted in the entire set divided by the total number of moves. We also considered training and validation loss when assessing if models over-fit.

As detailed in Section 4, we undertook a systematic exploration of the possibility space. The main five possibilities we considered, in order, were:

1. Learning Rate
2. Training Steps
3. Depth of Gradient Flow
4. Use of Random Initialization
5. Choice of Pretrained Model

We ordered the possibilities so that the correct choice of parameter should not be conditioned on the correct choice of the previous parameters.

As noted in the main text, we used the Tensorflow Keras [2, 12] stochastic gradient descent and momentum optimizer. We then started with the hyper-parameters used for training Maia, and used a grid search to determine the optimal choices.

A.2.1 Training Hyperparameters

The starting configuration of parameters was based on shortened schedule from the training code for the starting pretrained models. It did not perform well and we found the batch size should be significantly smaller; going from 1024 to 128 allowed us to get convergence. For this discussion we consider one step/iteration to be a single forward pass of a batch of inputs, followed by the backward pass. The learning rate was reduced by a factor of 10 thrice during these runs, once at step 200,000, then step 400,000, finally step 600,000, the total number of steps was 1,000,000. We also used the Maia targeting ELO 1900 as the starting model, and stopped the gradients at layer 3 (labeled *Start of policy head* in figure 1).

The summary of our initial exploration of possible learning rates (η) is shown in Table 1. Learning rate here refers to the initial learning rate, as all went through the same two stage reduction processes. Also note that we divided the training batches into 64-element ghost batches [30]. We also explored higher batch sizes 512 and 1024 and learning rates down to 10^{-7} , but they did not converge.

These results suggest the choice of learning rate and batch size do not cause much effect within this small range. In part, this is due to the ghost batches, which reduce the effects of increasing batch size and also due to the learning rate being reduced by a factor of 10 twice during training. We decided on using 256 and 0.01 as they were performed the best, but this does suggest that lower batch sizes could allow for faster convergence at only a small cost to final accuracy.

Batch Size	64	64	128	128,	256	256*	256
Learning Rate	0.001	0.01	0.01	0.001	0.1	0.01*	0.001
Validation Accuracy	0.649	0.637	0.655	0.661	0.662	0.671	0.657

**Final chosen value*

Table 1: Validation accuracy by learning rate and batch size

We also found that accuracy gains stopped well before the final step, so we ran the training with a much shorter number of steps (200,000) and learning rate reduction boundaries (35,000, 80,000, 110000) using the selected learning rate. These tests showed no improvement beyond 130,000 steps, along with no over-fitting becoming apparent even after the 200,000 steps. As a result, we chose 150,000 as our final step count. A summary of this is shown in Table 2.

Number of Training Steps	130,000	150,000*	200,000
Validation Accuracy	0.673	0.670	0.671

**Final chosen value*

Table 2: Validation accuracy by learning rate

A.2.2 Depth of Gradient Flow and use of Random Initialization

As discussed in the main text, determining where the gradients should stop during training was a key component of our fine-tuning. We set out 10 possible options: as shown in Figure 1, 9 options

Depth of Gradient Flow	1	2	3	4	5	6	7	8	9	No Stop*
Pretrained Initialization*	0.542	0.583	0.607	0.635	0.644	0.653	0.665	0.675	0.679	0.684
Random Initialization	0.542	0.587	0.604	0.618	0.632	0.634	0.638	0.638	0.640	0.628

*Final chosen value

Table 3: The effects of gradient flow depth and Model Initialization on validation accuracy

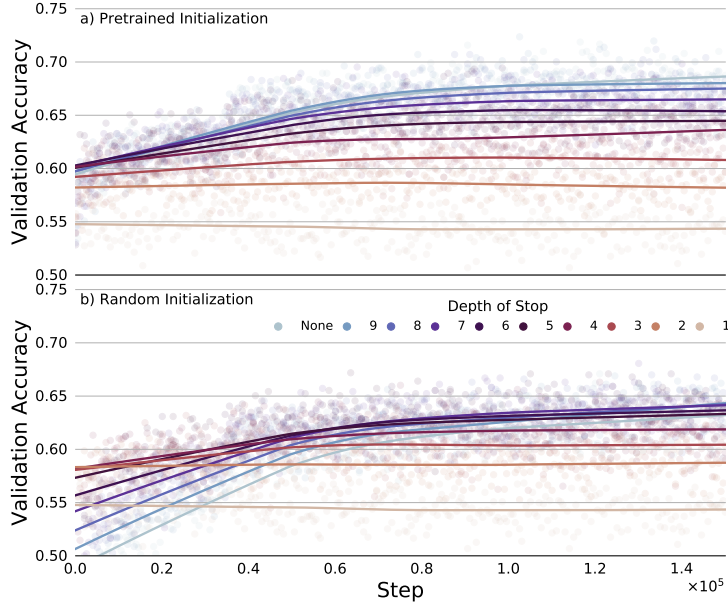


Figure 8: The effects of gradient flow depth and Model Initialization on validation accuracy

correspond to different layers in the model, and the 10th option is to not stop at all. They are ordered from the top down, where depth 2 corresponds to one layer being updated, while 5 means the first two layers plus two residual blocks are updated. Depth 1 has no weights to update. Table 3 and Figure 9 show how the depth of the gradient flow affects the resulting accuracy. We looked at two conditions for all options. First, we tested a pre-trained initialization, meaning our initial weights were the same Maia 1900 above and below the stop. Second, we tested a random initialization, where above the stop the weights were initialized randomly. As can be seen in Table 3, accuracy monotonically improves with the depth of gradient flow, for both pretrained and random initializations. Thus, the best fine-tuning procedure in our setting is to not freeze any layers at all. Also, the pretrained initialization outperformed the random initialization in virtually every test. These strong results for pretrained initialization with no stops is also supported by the larger test shown in Figure 2.

A.2.3 Choice of Pretrained Model

Our final consideration was how the choice of which pretrained model to start from affects accuracy. There are several pretrained models we could choose from, each trained on a separate population of players at a particular skill level. Interestingly, as shown in Table 4, the choice is not significant if the entire model is allowed to update during training (the no stop condition). The model does have a weak effect if only the top layers are used (the depth 3 condition). Therefore, we use the models trained on 1900 ELO as the starting point of all players.

Pretrained model targeted ELO	1100	1500	1800	1900*
No Stop*	0.679	0.680	0.678	0.684
Depth 3	0.586	0.605	0.609	0.607

*Final chosen value

Table 4: The effects of chosen starting model on validation accuracy. Each point is using a small sample (2560 boards) of the validation set, the lines are using a simple Lowess smoothing

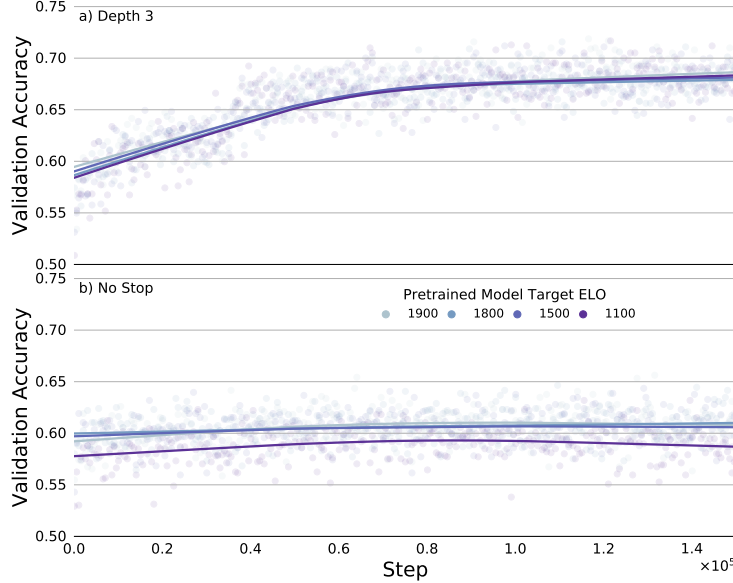


Figure 9: The effects of chosen starting model on validation accuracy. Each point is using a small sample (2560 boards) of the validation set, the lines are using a simple Lowess smoothing

A.2.4 Training Infrastructure and Duration

In this work the training was done on *Microsoft Azure* virtual machines using multiple *Tesla K80* GPUs. We trained 4 in parallel on each GPU, at a small cost in training time (about 16 to 20 hours training time). But to train a single model would take between 12 and 14 hours on the hardware.

A.3 Stylometry Details

In §5.2, we presented stylometry results for the full set of 398 players, showing that our personalized models can nearly perfectly identify a player by looking at just 4 games from their test set. To examine these results more closely, we also experiment with a smaller set of 30 players. Figure 10 summarizes the results, including the results reported in §5.2.

Figure 10(a) shows the stylometry accuracy among 30 players when the models are given access to a single game, while varying the subset of moves shown to the models. If all moves from the beginning up to move x are shown, the accuracy converges quickly to 90.8%; conversely, starting at move x and proceeding to the end of the game degrades accuracy gradually from 26.1% to 84.8%. The baselines in these plots are the Naive Bayes classifier and random guessing (described in §5.2), both of which perform poorly.

Identifying a player from a set of 30 is easier than identifying a player from a set of 398. Figure 10(c) shows the analogous results for the full set of 398 players. Although the curves have similar properties, the stylometry accuracy peaks at lower numbers and the baselines perform even worse than before. Recall, however, that we are only giving the models access to a *single* game. If instead we give them access to 4 games, then accuracy converges very quickly to nearly 100%, as shown in Figure 10(d).

To further investigate the effect of multiple games, we used the 30 player set and gave the models access to 4,000 games from each player’s test set. The results are shown in Figure 10(d). Interestingly, the stylometry accuracy reaches and *stays* at 100% regardless of which subset of moves is shown to the models. For example, showing only move x from each of the 4,000 games results in 100% stylometry accuracy, for any value of x that is higher than the first few moves (e.g., $x \geq 3$). Although the baselines perform better given the larger number of games, their accuracy never exceeds 13.5%.

By analyzing our stylometry accuracy in terms of the quality of a move, we can gain some insight into which moves are particularly useful in identifying players. Recall that we measure a move’s quality or “goodness” by the change in win probability it causes, where win probability is calculated via an

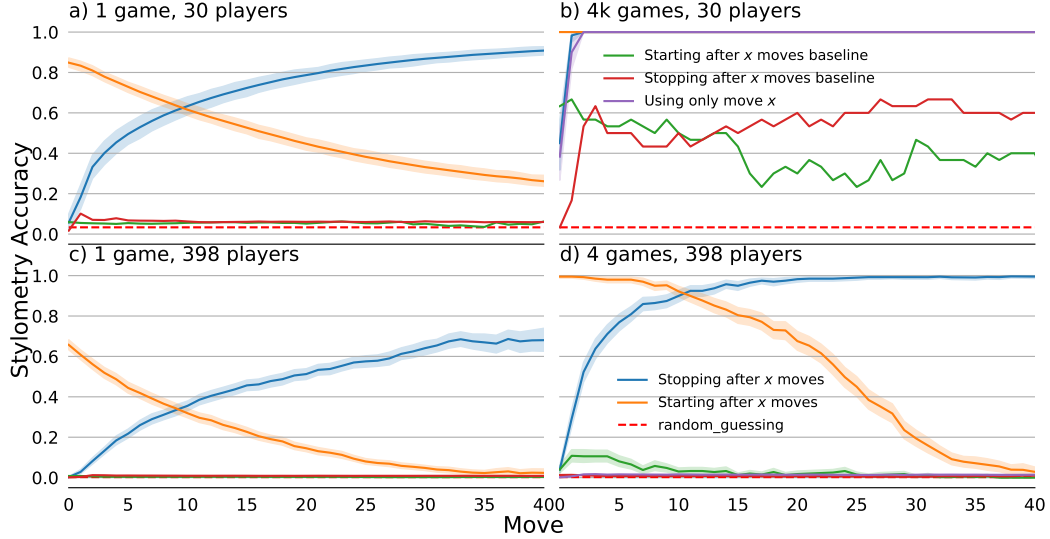


Figure 10: Stylometry accuracy (prediction accuracy of player identification) as a function of which moves the models are given, shown for a smaller 30 player set when using (a) 1 game and (b) 4,000 games, and on the full 398 player set when using (c) 1 game and (d) 4 games. Whereas our accuracy is nearly perfect given at least 4 games, all baselines (defined in §5.2) perform poorly, providing little benefit over random guessing except when given a large number of games in (b). *Stopping after x* means that only moves before move x are considered, while *Starting after x* means only moves after move x are used.

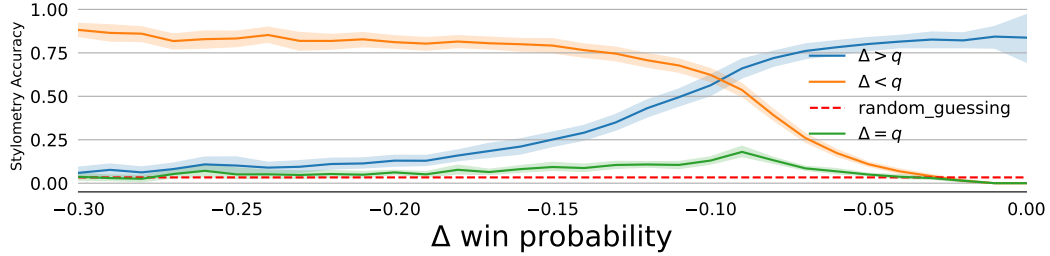


Figure 11: Stylometry accuracy as a function of the change in win probability of a move, shown for a 30 player set when using a single game. Change in win probability is always negative because it is measured against optimal play. Lower quality moves are less useful for identifying players than higher quality moves. $\Delta > q$ means that only moves with quality greater than q are considered, and similarly for the other lines.

empirical procedure based on the position’s centipawn score, following the method of McIlroy-Young et al. [43]. Figure 11 shows stylometry accuracy as a function of the change in win probability of a move. We see that looking at lower quality moves lead to lower stylometry accuracy than looking at higher quality moves. The sweet spot lies around a win probability change of -0.1 , which corresponds to a slight inaccuracy in chess. This suggests that small inaccuracies are a potentially good style marker for uniquely identifying players in chess.

A.4 Example Game

Here, we show stylometry being performed on a single game. For each player in our 398 player set, we run their personalized model on the game. Each model generates a move prediction for every move in the game. In Figure 12, each row corresponds to a personalized model, and each column corresponds to a move in the game. The cell is light if the model correctly predicted the move, and dark otherwise. The rows are sorted by prediction accuracy in descending order. The player who actually played the

game is the first row of the table, indicating that their model is the most accurate predictor of this game (and hence that we perform stylometry correctly in this case).

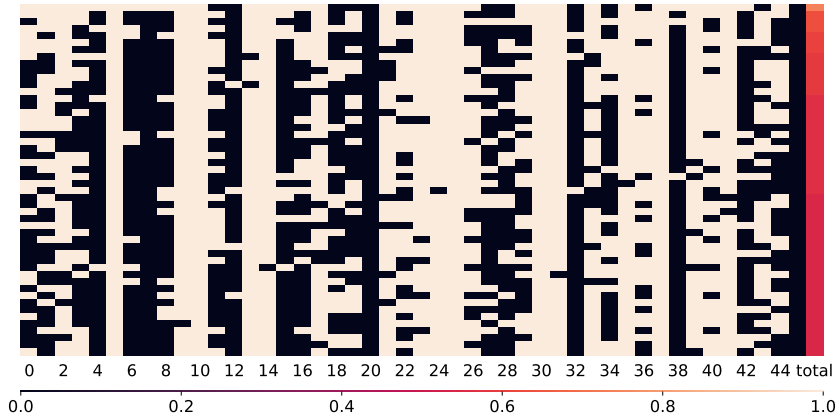


Figure 12: The correct player is 76% accurate while all others are 63% or below. These are the most accurate models in the rows with white indicating correct predictions on the moves (columns)

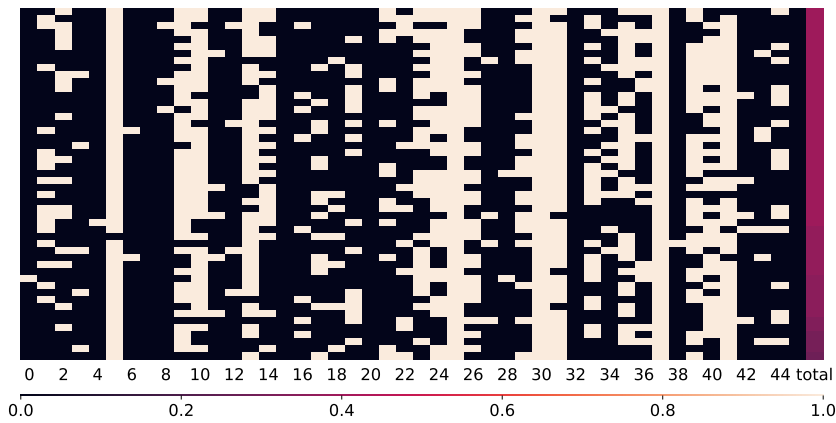


Figure 13: The worst player is 28% accurate while all others are 63% or below. These are the least accurate models in the rows with white indicating correct predictions on the moves (columns)

```

[Event "Rated Blitz game"]
[Site "https://lichess.org/-----"]
[Date "2020.05.31"]
[Round "-"]
[White ""]
[Black ""]
[Result "0-1"]
[Opening "Sicilian Defense: Bowdler Attack"]
[Termination "Time forfeit"]
[TimeControl "180+0"]

1. e4 c5 2. Bc4 Nc6 3. Nf3 e6 4. c3 a6 5. d4 d5 6. exd5 exd5 7. Bb3 Nf6 8. 0-0
h6 9. Re1+ Be6 10. dxc5 Bxc5 11. Nbd2 0-0 12. Nf1 Qb6 13. Be3 Ne4 14. Bxc5
Qxc5 15. Ne3 Rad8 16. Nd4 Rfe8 17. Rc1 Ne5 18. f3 Nf6 19. f4 Nc6 20. f5 Bd7
21. Qd3 Re5 22. Kh1 Rde8 23. Re2 Nxd4 24. Qxd4 Qxd4 25. cxd4 Rxe3 26. Rxe3
Rxe3 27. h3 Bxf5 28. Rc7 Be4 29. Rxb7 Rxh3+ 30. Kg1 Rg3 31. Rb8+ Kh7 32.
Rb7 Rg2+ 33. Kf1 Kg6 34. Rb6 Rxb2 35. Rxa6 Bd3+ 36. Ke1 Bxa6 37. Kd1 Bc4
38. Bxc4 dxc4 39. Kc1 c3 40. d5 Nxd5 41. a3 Ra2 42. a4 Rxa4 43. Kb1 Nb4 44.
Kc1 Ra2 45. Kb1 c2+ 46. Kc1 Kf5 0-1

```

Figure 14: PGN of the game used

A.5 Complete player data

AnonID	ELO	Total Games	Training Set Size	Validate Set Size	Test Set Size	First Game Played	Use
1	1100	44859	35889	4485	4485	2016	train
2	1300	49609	39689	4960	4960	2013	extended
3	1300	41818	33456	4181	4181	2015	extended
4	1400	45759	36609	4575	4575	2016	extended
5	1400	62406	49926	6240	6240	2013	extended
6	1400	42464	33972	4246	4246	2016	extended
7	1500	47957	38367	4795	4795	2016	extended
8	1500	44934	35948	4493	4493	2013	extended
9	1500	43568	34856	4356	4356	2016	train
10	1500	62079	49665	6207	6207	2016	extended
11	1600	42049	33641	4204	4204	2014	extended
12	1600	50240	40192	5024	5024	2017	train
13	1600	51315	41053	5131	5131	2014	extended
14	1700	60398	48320	6039	6039	2015	extended
15	1700	64483	51587	6448	6448	2014	extended
16	1700	79666	63734	7966	7966	2016	train
17	1800	52283	41827	5228	5228	2015	extended
18	1800	61448	49160	6144	6144	2014	extended
19	1800	46540	37232	4654	4654	2014	extended
20	1800	44164	35332	4416	4416	2016	train
21	1900	69137	55311	6913	6913	2014	train
22	1900	47176	37742	4717	4717	2015	extended
23	1900	43027	34423	4302	4302	2017	extended
24	1900	88007	70407	8800	8800	2016	extended
25	1900	59007	47207	5900	5900	2017	train
26	1900	44792	35834	4479	4479	2017	train
27	2000	70935	56749	7093	7093	2015	train
28	2000	52566	42054	5256	5256	2015	extended
29	2000	48564	38852	4856	4856	2016	train
30	2000	53162	42530	5316	5316	2015	extended

Table 5: Players in the Final Tuning analysis

AnonID	ELO	Total Games	Training Set Size	Validate Set Size	Test Set Size	First Game Played
1	1200	60590	48472	6059	6059	2016
2	1200	47144	37716	4714	4714	2016
3	1200	50081	40065	5008	5008	2016
4	1200	80413	64331	8041	8041	2016
5	1300	52215	41773	5221	5221	2016
6	1300	41818	33456	4181	4181	2015
7	1300	60989	48793	6098	6098	2016
8	1300	50247	40199	5024	5024	2013
9	1300	43475	34781	4347	4347	2015
10	1300	49609	39689	4960	4960	2013
11	1300	43983	35187	4398	4398	2017
12	1300	101106	80886	10110	10110	2015
13	1300	45214	36172	4521	4521	2018
14	1400	45759	36609	4575	4575	2016
15	1400	46832	37466	4683	4683	2016
16	1400	47657	38127	4765	4765	2016
17	1400	46915	37533	4691	4691	2014
18	1400	52982	42386	5298	5298	2015
19	1400	44133	35307	4413	4413	2014
20	1400	57679	46145	5767	5767	2016
21	1400	56211	44969	5621	5621	2016
22	1400	59989	47993	5998	5998	2017
23	1400	77993	62395	7799	7799	2017

24	1400	43574	34860	4357	4357	2015
25	1400	56619	45297	5661	5661	2015
26	1400	64311	51449	6431	6431	2017
27	1400	42182	33746	4218	4218	2017
28	1400	127974	102380	12797	12797	2017
29	1400	41833	33467	4183	4183	2018
30	1400	48301	38641	4830	4830	2013
31	1400	42348	33880	4234	4234	2017
32	1400	92484	73988	9248	9248	2015
33	1500	42628	34104	4262	4262	2016
34	1500	44700	35760	4470	4470	2016
35	1500	72152	57722	7215	7215	2016
36	1500	44721	35777	4472	4472	2016
37	1500	49109	39289	4910	4910	2014
38	1500	51179	40945	5117	5117	2015
39	1500	45874	36700	4587	4587	2014
40	1500	97073	77659	9707	9707	2013
41	1500	55801	44641	5580	5580	2016
42	1500	51793	41435	5179	5179	2015
43	1500	46824	37460	4682	4682	2016
44	1500	55941	44753	5594	5594	2017
45	1500	42017	33615	4201	4201	2017
46	1500	51368	41096	5136	5136	2016
47	1500	47025	37621	4702	4702	2015
48	1500	47427	37943	4742	4742	2016
49	1500	59320	47456	5932	5932	2016
50	1500	52451	41961	5245	5245	2016
51	1500	47728	38184	4772	4772	2014
52	1500	48409	38729	4840	4840	2015
53	1500	50935	40749	5093	5093	2013
54	1500	57666	46134	5766	5766	2017
55	1500	47957	38367	4795	4795	2016
56	1500	45638	36512	4563	4563	2017
57	1500	59350	47480	5935	5935	2015
58	1500	45296	36238	4529	4529	2017
59	1600	43470	34776	4347	4347	2016
60	1600	43209	34569	4320	4320	2014
61	1600	47428	37944	4742	4742	2016
62	1600	54993	43995	5499	5499	2016
63	1600	51786	41430	5178	5178	2016
64	1600	69134	55308	6913	6913	2016
65	1600	72079	57665	7207	7207	2015
66	1600	45610	36488	4561	4561	2017
67	1600	43494	34796	4349	4349	2015
68	1600	43690	34952	4369	4369	2017
69	1600	152342	121874	15234	15234	2015
70	1600	114035	91229	11403	11403	2015
71	1600	48663	38931	4866	4866	2015
72	1600	48929	39145	4892	4892	2013
73	1600	43750	35000	4375	4375	2015
74	1600	48124	38500	4812	4812	2015
75	1600	43922	35138	4392	4392	2016
76	1600	42148	33720	4214	4214	2016
77	1600	47934	38348	4793	4793	2014
78	1600	49252	39402	4925	4925	2015
79	1600	50547	40439	5054	5054	2014
80	1600	131602	105282	13160	13160	2013
81	1600	42628	34104	4262	4262	2016
82	1600	43194	34556	4319	4319	2017

83	1600	70398	56320	7039	7039	2013
84	1600	45333	36267	4533	4533	2017
85	1600	46061	36849	4606	4606	2016
86	1600	55568	44456	5556	5556	2015
87	1600	43925	35141	4392	4392	2014
88	1600	57713	46171	5771	5771	2016
89	1600	57126	45702	5712	5712	2017
90	1600	52403	41923	5240	5240	2014
91	1600	67655	54125	6765	6765	2016
92	1600	54504	43604	5450	5450	2013
93	1600	45539	36433	4553	4553	2015
94	1600	61852	49482	6185	6185	2016
95	1600	74944	59956	7494	7494	2015
96	1600	51315	41053	5131	5131	2014
97	1600	42505	34005	4250	4250	2015
98	1600	56503	45203	5650	5650	2014
99	1600	70757	56607	7075	7075	2015
100	1600	50168	40136	5016	5016	2013
101	1600	43711	34969	4371	4371	2016
102	1600	54595	43677	5459	5459	2015
103	1600	44172	35338	4417	4417	2015
104	1600	78644	62916	7864	7864	2013
105	1600	66119	52897	6611	6611	2015
106	1600	43185	34549	4318	4318	2014
107	1600	49080	39264	4908	4908	2015
108	1600	43943	35155	4394	4394	2015
109	1600	89451	71561	8945	8945	2015
110	1600	71746	57398	7174	7174	2015
111	1600	45879	36705	4587	4587	2016
112	1600	57919	46337	5791	5791	2017
113	1600	46858	37488	4685	4685	2017
114	1600	49645	39717	4964	4964	2016
115	1600	48892	39114	4889	4889	2017
116	1600	52053	41643	5205	5205	2017
117	1600	88602	70882	8860	8860	2015
118	1600	44881	35905	4488	4488	2016
119	1700	61927	49543	6192	6192	2013
120	1700	105998	84800	10599	10599	2015
121	1700	76328	61064	7632	7632	2016
122	1700	50437	40351	5043	5043	2018
123	1700	63791	51033	6379	6379	2014
124	1700	52538	42032	5253	5253	2013
125	1700	50054	40044	5005	5005	2017
126	1700	43268	34616	4326	4326	2018
127	1700	48561	38849	4856	4856	2015
128	1700	44522	35618	4452	4452	2016
129	1700	78571	62857	7857	7857	2016
130	1700	131802	105442	13180	13180	2015
131	1700	77154	61724	7715	7715	2013
132	1700	47852	38282	4785	4785	2017
133	1700	51350	41080	5135	5135	2016
134	1700	42296	33838	4229	4229	2014
135	1700	42264	33812	4226	4226	2017
136	1700	49008	39208	4900	4900	2016
137	1700	42277	33823	4227	4227	2015
138	1700	53367	42695	5336	5336	2016
139	1700	45667	36535	4566	4566	2016
140	1700	61285	49029	6128	6128	2015
141	1700	43765	35013	4376	4376	2018

142	1700	101501	81201	10150	10150	2016
143	1700	77249	61801	7724	7724	2015
144	1700	47421	37937	4742	4742	2016
145	1700	66504	53204	6650	6650	2015
146	1700	41850	33480	4185	4185	2016
147	1700	52988	42392	5298	5298	2017
148	1700	42977	34383	4297	4297	2015
149	1700	50553	40443	5055	5055	2014
150	1700	42395	33917	4239	4239	2014
151	1700	49073	39259	4907	4907	2013
152	1700	46138	36912	4613	4613	2014
153	1700	65018	52016	6501	6501	2015
154	1700	64483	51587	6448	6448	2014
155	1700	60398	48320	6039	6039	2015
156	1700	66061	52849	6606	6606	2015
157	1700	63073	50459	6307	6307	2013
158	1700	52457	41967	5245	5245	2015
159	1700	78876	63102	7887	7887	2014
160	1700	66193	52955	6619	6619	2016
161	1700	77713	62171	7771	7771	2016
162	1700	53659	42929	5365	5365	2016
163	1700	53860	43088	5386	5386	2017
164	1700	43683	34947	4368	4368	2018
165	1700	64032	51226	6403	6403	2013
166	1700	49874	39900	4987	4987	2014
167	1700	53993	43195	5399	5399	2015
168	1700	42775	34221	4277	4277	2017
169	1700	54600	43680	5460	5460	2015
170	1700	56198	44960	5619	5619	2016
171	1700	54512	43610	5451	5451	2016
172	1700	43765	35013	4376	4376	2016
173	1700	46054	36844	4605	4605	2014
174	1700	56852	45482	5685	5685	2014
175	1700	56228	44984	5622	5622	2014
176	1700	107733	86187	10773	10773	2015
177	1700	45024	36020	4502	4502	2016
178	1700	46444	37156	4644	4644	2013
179	1700	41782	33426	4178	4178	2015
180	1700	59343	47475	5934	5934	2016
181	1700	76191	60953	7619	7619	2015
182	1700	49658	39728	4965	4965	2016
183	1700	47672	38138	4767	4767	2014
184	1700	50936	40750	5093	5093	2016
185	1700	45249	36201	4524	4524	2015
186	1700	46535	37229	4653	4653	2014
187	1700	42152	33722	4215	4215	2017
188	1700	68113	54491	6811	6811	2016
189	1700	42831	34265	4283	4283	2016
190	1700	73401	58721	7340	7340	2015
191	1700	71164	56932	7116	7116	2016
192	1700	42207	33767	4220	4220	2015
193	1700	50047	40039	5004	5004	2017
194	1700	46544	37236	4654	4654	2014
195	1700	45782	36626	4578	4578	2013
196	1700	46625	37301	4662	4662	2013
197	1700	53866	43094	5386	5386	2015
198	1700	53528	42824	5352	5352	2015
199	1700	49867	39895	4986	4986	2017
200	1700	67857	54287	6785	6785	2015

201	1700	47861	38289	4786	4786	2013
202	1700	53552	42842	5355	5355	2013
203	1700	48861	39089	4886	4886	2016
204	1700	70352	56282	7035	7035	2017
205	1700	48002	38402	4800	4800	2015
206	1700	46070	36856	4607	4607	2016
207	1700	49269	39417	4926	4926	2014
208	1700	62595	50077	6259	6259	2014
209	1700	41897	33519	4189	4189	2014
210	1700	44560	35648	4456	4456	2013
211	1700	42628	34104	4262	4262	2016
212	1700	54932	43946	5493	5493	2016
213	1800	42232	33786	4223	4223	2016
214	1800	41962	33570	4196	4196	2016
215	1800	46610	37288	4661	4661	2013
216	1800	69083	55267	6908	6908	2013
217	1800	43962	35170	4396	4396	2013
218	1800	47613	38091	4761	4761	2016
219	1800	64403	51523	6440	6440	2016
220	1800	42819	34257	4281	4281	2016
221	1800	52248	41800	5224	5224	2015
222	1800	64276	51422	6427	6427	2016
223	1800	61160	48928	6116	6116	2014
224	1800	57345	45877	5734	5734	2016
225	1800	41924	33540	4192	4192	2015
226	1800	47266	37814	4726	4726	2016
227	1800	54672	43738	5467	5467	2016
228	1800	58634	46908	5863	5863	2016
229	1800	58271	46617	5827	5827	2014
230	1800	53288	42632	5328	5328	2016
231	1800	56925	45541	5692	5692	2014
232	1800	64958	51968	6495	6495	2014
233	1800	71681	57345	7168	7168	2018
234	1800	53869	43097	5386	5386	2015
235	1800	64576	51662	6457	6457	2013
236	1800	78315	62653	7831	7831	2014
237	1800	47157	37727	4715	4715	2015
238	1800	41765	33413	4176	4176	2017
239	1800	60864	48692	6086	6086	2015
240	1800	46637	37311	4663	4663	2017
241	1800	52517	42015	5251	5251	2015
242	1800	61226	48982	6122	6122	2013
243	1800	66719	53377	6671	6671	2013
244	1800	43278	34624	4327	4327	2017
245	1800	53628	42904	5362	5362	2016
246	1800	49358	39488	4935	4935	2015
247	1800	54515	43613	5451	5451	2013
248	1800	88666	70934	8866	8866	2015
249	1800	71753	57403	7175	7175	2013
250	1800	42536	34030	4253	4253	2017
251	1800	63370	50696	6337	6337	2017
252	1800	42232	33786	4223	4223	2016
253	1800	92361	73889	9236	9236	2013
254	1800	53753	43003	5375	5375	2016
255	1800	45158	36128	4515	4515	2018
256	1800	46439	37153	4643	4643	2016
257	1800	53661	42929	5366	5366	2015
258	1800	78756	63006	7875	7875	2013
259	1800	125770	100616	12577	12577	2013

260	1800	77061	61649	7706	7706	2013
261	1800	44729	35785	4472	4472	2017
262	1800	77302	61842	7730	7730	2013
263	1800	54366	43494	5436	5436	2015
264	1800	46943	37555	4694	4694	2015
265	1800	61733	49387	6173	6173	2017
266	1800	45582	36466	4558	4558	2015
267	1800	41946	33558	4194	4194	2015
268	1800	45778	36624	4577	4577	2013
269	1800	55018	44016	5501	5501	2014
270	1800	78722	62978	7872	7872	2013
271	1800	42114	33692	4211	4211	2016
272	1800	49133	39307	4913	4913	2014
273	1800	43785	35029	4378	4378	2016
274	1800	45686	36550	4568	4568	2016
275	1800	43585	34869	4358	4358	2016
276	1800	49115	39293	4911	4911	2016
277	1800	54633	43707	5463	5463	2017
278	1800	44157	35327	4415	4415	2013
279	1800	60144	48116	6014	6014	2016
280	1800	71677	57343	7167	7167	2016
281	1800	80059	64049	8005	8005	2016
282	1800	68943	55155	6894	6894	2016
283	1800	54373	43499	5437	5437	2016
284	1800	63161	50529	6316	6316	2014
285	1800	51426	41142	5142	5142	2013
286	1800	44449	35561	4444	4444	2015
287	1800	55729	44585	5572	5572	2014
288	1800	46987	37591	4698	4698	2016
289	1800	63181	50545	6318	6318	2014
290	1800	55658	44528	5565	5565	2016
291	1800	43957	35167	4395	4395	2017
292	1800	50888	40712	5088	5088	2016
293	1800	50364	40292	5036	5036	2014
294	1800	60781	48625	6078	6078	2017
295	1800	58667	46935	5866	5866	2014
296	1800	51365	41093	5136	5136	2016
297	1800	48556	38846	4855	4855	2015
298	1800	41785	33429	4178	4178	2015
299	1800	46122	36898	4612	4612	2016
300	1800	42386	33910	4238	4238	2015
301	1800	42291	33833	4229	4229	2017
302	1800	47560	38048	4756	4756	2016
303	1800	57562	46050	5756	5756	2014
304	1900	59264	47412	5926	5926	2016
305	1900	47128	37704	4712	4712	2017
306	1900	50982	40786	5098	5098	2013
307	1900	43514	34812	4351	4351	2017
308	1900	53759	43009	5375	5375	2016
309	1900	76401	61121	7640	7640	2014
310	1900	64430	51544	6443	6443	2015
311	1900	50543	40435	5054	5054	2014
312	1900	48060	38448	4806	4806	2017
313	1900	51455	41165	5145	5145	2016
314	1900	48748	39000	4874	4874	2017
315	1900	89333	71467	8933	8933	2015
316	1900	47364	37892	4736	4736	2012
317	1900	61527	49223	6152	6152	2017
318	1900	60236	48190	6023	6023	2013

319	1900	50565	40453	5056	5056	2014
320	1900	49685	39749	4968	4968	2015
321	1900	42881	34305	4288	4288	2016
322	1900	45225	36181	4522	4522	2013
323	1900	63940	51152	6394	6394	2016
324	1900	48903	39123	4890	4890	2014
325	1900	53998	43200	5399	5399	2016
326	1900	52770	42216	5277	5277	2014
327	1900	52032	41626	5203	5203	2016
328	1900	46193	36955	4619	4619	2013
329	1900	47493	37995	4749	4749	2017
330	1900	55883	44707	5588	5588	2015
331	1900	82556	66046	8255	8255	2014
332	1900	77548	62040	7754	7754	2017
333	1900	54012	43210	5401	5401	2014
334	1900	49423	39539	4942	4942	2017
335	1900	43414	34732	4341	4341	2016
336	1900	49012	39210	4901	4901	2016
337	1900	45906	36726	4590	4590	2017
338	1900	61131	48905	6113	6113	2015
339	1900	49851	39881	4985	4985	2017
340	1900	44444	35556	4444	4444	2015
341	1900	71945	57557	7194	7194	2016
342	1900	46153	36923	4615	4615	2013
343	1900	53585	42869	5358	5358	2015
344	1900	69465	55573	6946	6946	2013
345	1900	50222	40178	5022	5022	2016
346	1900	53412	42730	5341	5341	2015
347	1900	62524	50020	6252	6252	2016
348	1900	45540	36432	4554	4554	2018
349	1900	47067	37655	4706	4706	2014
350	1900	46847	37479	4684	4684	2014
351	1900	46081	36865	4608	4608	2015
352	1900	78704	62964	7870	7870	2013
353	1900	91132	72906	9113	9113	2013
354	1900	53797	43039	5379	5379	2017
355	1900	51138	40912	5113	5113	2013
356	1900	46886	37510	4688	4688	2016
357	1900	67116	53694	6711	6711	2014
358	1900	42749	34201	4274	4274	2013
359	1900	44034	35228	4403	4403	2014
360	1900	53036	42430	5303	5303	2014
361	1900	47438	37952	4743	4743	2014
362	1900	45827	36663	4582	4582	2015
363	1900	59782	47826	5978	5978	2015
364	1900	52067	41655	5206	5206	2014
365	1900	82423	65939	8242	8242	2014
366	1900	49884	39908	4988	4988	2014
367	1900	51883	41507	5188	5188	2016
368	1900	47452	37962	4745	4745	2013
369	1900	55535	44429	5553	5553	2016
370	1900	44776	35822	4477	4477	2015
371	1900	118810	95048	11881	11881	2014
372	1900	71054	56844	7105	7105	2013
373	1900	48292	38634	4829	4829	2016
374	1900	124768	99816	12476	12476	2013
375	1900	55493	44395	5549	5549	2015
376	1900	50003	40003	5000	5000	2016
377	2000	47389	37913	4738	4738	2016

378	2000	43776	35022	4377	4377	2015
379	2000	44175	35341	4417	4417	2016
380	2000	71418	57136	7141	7141	2013
381	2000	44315	35453	4431	4431	2014
382	2000	43948	35160	4394	4394	2014
383	2000	52212	41770	5221	5221	2015
384	2000	51985	41589	5198	5198	2014
385	2000	47277	37823	4727	4727	2014
386	2000	50252	40202	5025	5025	2017
387	2000	49506	39606	4950	4950	2015
388	2000	48281	38625	4828	4828	2014
389	2000	96101	76881	9610	9610	2013
390	2000	56717	45375	5671	5671	2014
391	2000	49722	39778	4972	4972	2016
392	2000	43468	34776	4346	4346	2016
393	2000	50687	40551	5068	5068	2017
394	2000	49398	39520	4939	4939	2016
395	2000	43977	35183	4397	4397	2016
396	2000	52366	41894	5236	5236	2017
397	2000	46428	37144	4642	4642	2015
398	2000	52566	42054	5256	5256	2015

Table 6: Players in the main analysis, players shown with ELO 2000 are all rounded up from 1950+, none are above 2000